

# Determination of the Ionization State of 11-Thioundecyl-1-phosphonic Acid in Self-Assembled Monolayers by Chemical Force Microscopy

Jin Zhang, Jennifer Kirkham, and Colin Robinson

*Division of Oral Biology, Leeds Dental Institute, University of Leeds, Leeds, U.K.*

Mark L. Wallwork and D. Alastair Smith\*

*Department of Physics and Astronomy, University of Leeds, Leeds, U.K.*

Andrew Marsh and Michael Wong

*Department of Chemistry, University of Warwick, Coventry, U.K.*

**The present article describes the preparation and preliminary characterization of a novel phosphate-functionalized self-assembled monolayer (SAM) and the determination of the surface ionization states of the phosphate headgroup in aqueous solutions by chemical force microscopy (CFM). The phosphate headgroup used was PO(OH)<sub>2</sub>, a diprotic acid. The adhesion force between an AFM probe and a flat substrate, both of which were chemically modified with the same phosphate SAM, was also measured as a function of pH and ionic strength. At low ionic strength (10<sup>-4</sup> M), two peaks were observed in the force titration curve (adhesion force versus pH) at pH 4.5 and 8.4. The two peaks are positioned 2.4 and 1.2 pH units higher, respectively, than the acid dissociation constants obtained for the phosphate group free in aqueous solution. At high ionic strength (10<sup>-1</sup> M), the adhesion forces were reduced by 1 order of magnitude and the peaks were replaced by shoulders similar to those previously reported for acid force titrations. On the basis of JKR theory, the surface p*K*<sub>a</sub> values of the phosphate group in high ionic strength solutions were found to be 4.5 and 7.7, respectively. However, in light of the effects of ionic strength on the force titration curves, we discuss the applicability of JKR theory to nanoscopic measurements of adhesion force and surface p*K*<sub>a</sub>.**

Intermolecular forces at surfaces on the micro- and nanometer scale are central to a wide range of biological, chemical, and physical processes (e.g., heterogeneous catalysis, colloidal chemistry, adhesives, lubrication, membrane transport, molecular recognition, cell signaling, and control of skeletal tissue mineral growth<sup>1–8</sup>). The principle interactions that play a role in controlling these phenomena include van der Waals forces and hydrogen-

bonding and electrostatic charge interactions,<sup>1,6,7</sup> and in many processes these interactions are highly specific. For example, the work of Fersht<sup>5</sup> and Creighton<sup>9</sup> has shown that a change in the ionization state of a single functional group in a biomolecule can dramatically affect its interaction with neighboring groups and lead to a major change in its overall structure. Since many biological processes take place in aqueous media on or near surfaces, the ability to measure and interpret intermolecular surface interactions and ionization states under aqueous conditions should contribute significantly to our understanding of biomolecular structure and function.

A key feature of the chemistry of surfaces is the difference in the behavior of ionizable groups resident on those surfaces compared with their behavior free in solution. While surface-specific techniques such as contact angle measurements are able to probe the surface p*K*<sub>a</sub> values of ionizable groups,<sup>1</sup> they are unable to map the distribution of such groups over a surface with anything approaching molecular resolution. However, the development of local probe techniques such as atomic force microscopy (AFM) during the past fifteen years has created new possibilities for the study of interfacial phenomena close to the atomic level.<sup>10</sup> Very recently, “chemical force microscopy” (CFM) has been

- (1) Israelachvili, J. *Intermolecular and Surface Force*, 2nd ed.; Academic Press: London, 1997.
- (2) Ulman, A. *An introduction to Ultrathin Organic Films: from Langmuir-Blodgett to Self-Assembly*; Academic Press: San Diego, CA, 1991.
- (3) Kendall, K. *Science* **1994**, *263*, 1720–1726.
- (4) Feng, S.; Chen, J. K.; Yu, H.; Simon, J. A.; Schreiber, S. L. *Science* **1994**, *266*, 1241–1246.
- (5) Fersht, T. *Enzyme Structure and Mechanics*; W. H. Freeman: New York, 1985.
- (6) Noy, A.; Frisbie, C. D.; Rozsnyai, L. F.; Wrighton, M. S.; Lieber, C. M. *J. Am. Chem. Soc.* **1995**, *117*, 7943–7951.
- (7) Vezenov, D. V.; Noy, A.; Rozsnyai, L. F.; Lieber, C. M. *J. Am. Chem. Soc.* **1997**, *119*, 2006–2015.
- (8) Robinson, C.; Kirkham, J.; Shore, R. *Dental Enamel, Formation to Destruction*; CRC Press: London, 1995.
- (9) Creighton, T. E. *Proteins: Structure and Molecular Properties*, 2nd ed.; W. H. Freeman: New York, 1993.

\* Corresponding author: (e-mail) d.a.m.smith@leeds.ac.uk; (fax) +113 233 3900.

introduced as a new AFM mode of operation in which the AFM tips are chemically modified to have a specific functionality by the covalent attachment of a molecular monolayer.<sup>6,7,11–13</sup> An extension of this technique, the “force titration”, in which the tip–sample interaction is monitored as a function of pH,<sup>7,13–20</sup> can be used to determine and map surface  $pK_a$  with nanometer resolution. Critical to the development of the technique is the availability of well-characterized model surfaces, and therefore, the design and fabrication of thin molecular films that simulate the chemistry of biological surfaces is extremely important and is the subject of this present report.

A particularly important molecular group in biology is the phosphate group. Phosphates occur at the surface of phosphorylated proteins, in nucleic acids, and in cell membranes. Often phosphorylation or dephosphorylation of proteins is a controlling factor in the determination of protein conformation. More specifically in skeletal tissue, interactions between extracellular matrixes and the mineral phase, calcium hydroxyapatite, are thought to be mediated by phosphate groups.<sup>8</sup> These interactions are considered to be important in both initiating and modulating skeletal crystal growth.

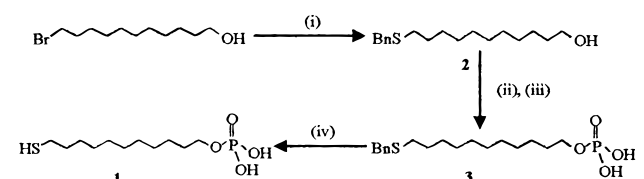
To investigate the behavior of surface-immobilized phosphate groups, we have synthesized and prepared self-assembled monolayers (SAMs) with a phosphate headgroup. Here we report on the synthesis and characterization of this novel  $\omega$ -functionalized alkanethiol and present CFM force–titration curves for probes and substrates both modified with the phosphate SAM. In this way, the surface ionization states of the phosphate headgroup and the ionic strength dependence of the surface  $pK_a$  have been determined.

## EXPERIMENTAL SECTION

Solvents used in this study were reagent grade or better, and in particular, the solvents used in substrate and probe functionalization were HPLC grade to reduce particulate matter. Ultrapure water with a resistivity of above 18 M $\Omega$ ·cm was used throughout the experiments. Constant ionic strength phosphate buffer solutions at different pH values were prepared according to methods reported in the literature.<sup>7,21</sup>

**Synthesis of 11-Thioundecyl-1-phosphonic Acid.** We chose phosphonic acid **1** (Scheme 1) as a target for synthesis because

Scheme 1. Synthesis of 11-Thioundecyl-1-phosphonic Acid<sup>a</sup>



<sup>a</sup>Conditions: (i) BnSH (85%); (ii) POCl<sub>3</sub>, Et<sub>3</sub>N THF; (iii) NaHCO<sub>3</sub> (aq) (65%); (iv) Na, NH<sub>3</sub> (l) (62%).

the alkyl chain is long enough to form regular SAMs on the gold surface. 11-Bromoundecanol was reacted with benzyl mercaptan to give the corresponding benzyl thioether **2**. Phosphorylation was then accomplished with phosphorus oxychloride,<sup>22</sup> to give, after partial hydrolysis, phosphonic acid **3**. The thiol was then synthesized by deprotection of the benzyl group using sodium in liquid ammonia, giving **1** in good yield, and its structure was confirmed with FAB-MS, <sup>1</sup>H NMR and FT-IR.<sup>23</sup>

Benzyl mercaptan and 11-bromoundecanol were purchased from Aldrich Chemical Co. Solvents and reagents were used as received. Flash column chromatography was performed on Merck silica gel (No. 109385), and TLC was carried out on precoated plates (silica gel 60 F254, Merck No. 5715). The products were visualized using UV light or potassium permanganate dip as appropriate. <sup>1</sup>H NMR spectra were acquired using a Bruker 250-MHz instrument, and chemical shifts are relative to tetramethylsilane. Mass spectra were recorded on a VG instrument and microanalyses were carried out by Warwick Analytical Services.

**(i) Preparation of 11-Benzylthioundecanol.** Sodium (1.01 g, 43.8 mmol, 1.1 equiv) was added to dry ethanol (40 mL) at 0 °C. Benzyl mercaptan (4.7 mL, 4.94 g, 39.81 mmol, 1 equiv) was added via syringe, followed by a solution of 11-bromo-1-undecanol (10 g, 39.81 mmol) in dry ethanol (20 mL), and the reaction mixture refluxed overnight. The mixture was cooled, poured into saturated ammonium chloride solution (100 mL), and then extracted with chloroform (3 × 50 mL). The combined organic phases were dried with magnesium sulfate and filtered and the solvent evaporated under reduced pressure to give a yellow oil which solidified after 1 h at room temperature. The crude product was dissolved in ether (200 mL) and the white precipitate removed by filtration. The organic phase was concentrated under reduced pressure to give the 11-benzylthioundecanol as a yellow solid (9.95 g, 85%).

**(ii, iii) Preparation of 11-Benzylthioundecyl-1-phosphonic Acid.** To a stirred solution of phosphorus oxychloride (0.815 mL, 1.34 g, 8.74 mmol, 1.3 equiv) in dry THF (30 mL) at 0 °C was added triethylamine (1.42 mL, 1.03 g, 10.19 mmol, 1.5 equiv) dropwise via syringe, and the resultant mixture was stirred for 10 min until a white precipitate appeared. After a further 10 min stirring, a solution of 11-benzylthioundecanol (1.98 g, 6.72 mmol) was added to the reaction via dropping funnel over a period of 20

- (10) (a) Marti, O.; Ribi, H. O.; Drake, B.; Albrecht, T. R.; Duate, C. F.; Hansma, P. K. *Science* **1988**, *239*, 50–54. (b) Formmer, J. *Angew. Chem., Int. Ed. Engl.* **1992**, *31*, 1298–1304. (c) Mate, C. M.; McClelland, G. M.; Erlandsson, R.; Chiang, S. *Phys. Rev. Lett.* **1987**, *59*, 1942–1945.
- (11) Frisbie, C. D.; Rozsnyai, L. F.; Noy, A.; Wrighton, M. S.; Lieber, C. M. *Science* **1994**, *265*, 2071–2076.
- (12) Green, J.-B. D.; McDermott, M. T.; Porter, M. D.; Siperko, L. M. *J. Phys. Chem.* **1995**, *99*, 10960–10965.
- (13) Takano, H.; Kenseth, J. R.; Wong, S.-S.; O'Brien, J. C.; Porter, M. D. *Chem. Rev.* **1999**, *99*, 2845–2890.
- (14) He, H. X.; Li, C. Z.; Song, J. Q.; Mu, T.; Wang, L.; Zhang, H. L.; Liu, Z. F. *Mol. Cryst. Liq. Cryst.* **1997**, *A294–295*, 99–102.
- (15) Van der Vegte, E. W.; Hadziioannou, G. *Langmuir* **1997**, *13*, 4357–4362.
- (16) Zhang, H.; He, H. X.; Mu, T.; Liu, Z. F. *Appl. Phys.* **1998**, *A66*, S269.
- (17) Hu, K.; Bard, A. J. *Langmuir* **1997**, *13*, 5114–5119.
- (18) Ito, T.; Namba, M.; Buhlmann, P.; Umezawa, Y. *Langmuir*, **1997**, *13*, 4323–4332.
- (19) Zhang, H.; He, H. X.; Mu, T.; Liu, Z. F. *Thin Solid Films* **1998**, *778*, 327–329.
- (20) Zhang, H.; Zhang, H. L.; He, H. X.; Zhu, T.; Liu, Z. F. *Mater. Sci. Eng. C*, **1999**, *8–9*, 191–194.
- (21) *CRC Handbook of Chemistry and Physics*, 72nd ed.; Lide, D. R., Ed.; CRC Press: Boca Raton, FL, 1991.

- (22) *Phosphorous oxychloride*: toxic by inhalation and contact with skin, irritant, reacts violently with water. *Liquid ammonia*: toxic by inhalation and contact with skin, irritant, flammable. *Sodium metal*: reacts violently with water; releases extremely flammable gas upon contact with water.
- (23) Spectral data of **1**: <sup>1</sup>H NMR (250 MHz, CDCl<sub>3</sub>),  $\delta$  4.04 (2H, q, CH<sub>2</sub>O), 3.56 (2H, br, m, P(OH)<sub>2</sub>), 2.50 (2H, t, SCH<sub>2</sub>CH<sub>2</sub>), 1.80–1.10 (18H, m, CH<sub>2</sub>); FT-IR,  $\nu_{\max}$  (solid) 3120, 2923, 2850 (C–H), 2539 (S–H), 1465, 1140 (P=O), 1034 (P–O–C) cm<sup>-1</sup>; MS (FAB) M + 1, 285.

min and the resultant mixture allowed to stir for 90 min at room temperature. The reaction was monitored by TLC, eluting with 10% methanol/chloroform. Saturated aqueous hydrogen carbonate (60 mL) was added to the reaction and left for 48 h. The mixture was diluted with water (50 mL) and washed with chloroform (60 mL). The aqueous phase was acidified to pH 1 with 1 M hydrochloric acid (~5 mL) and the product extracted with diethyl ether (4 × 50 mL), dried with magnesium sulfate, filtered, and evaporated under reduced pressure to give a yellow solid. The crude material was purified by flash column chromatography (eluent chloroform to 10% methanol/chloroform) to give the 11-benzylthioundecyl-1-phosphonic acid as a white solid (1.65 g, 65%).

**(iv) Preparation of 11-Thioundecyl-1-phosphonic Acid.**

To liquid ammonia (50 mL) in a flask fitted with a dry ice condenser was added small pieces of sodium (~1 g, excess) sufficient to obtain a permanent blue coloration and the solution cooled to -78 °C. A solution of phosphonic acid **3** (0.5 g, 1.337 mmol) in dry THF (15 mL) was added via syringe, and the reaction was stirred at low temperature for 1 h and then allowed to warm to reflux for a further 1 h. The reaction mixture was recooled to -78 °C and quenched cautiously with wet THF (15 mL). The reaction was allowed to warm to 0 °C, and the dry ice condenser was removed after 10 min. Saturated ammonium chloride solution (15 mL) was added cautiously under nitrogen and the mixture left to stir for 30 min at room temperature before it was acidified to pH 1 with 2 M hydrochloric acid (~15 mL). The product was extracted into chloroform (3 × 50 mL), dried with magnesium sulfate, filtered, and evaporated under reduced pressure to yield the 11-thioundecyl-1-phosphonic acid as a white solid (0.401 g, 62%).

**Probe Tips and Substrates.** Ultraflat gold-coated silicon substrates were prepared using the template stripping method.<sup>24</sup> A clean silicon wafer surface was coated with 150 nm of gold by thermal evaporation in an Edwards Auto 306 TMP vacuum evaporator. A clean glass slide was bonded to the gold-coated surface of the silicon wafer with EPO-Tek 377 adhesive (Promatech) and cured at 140 °C for 1 h. The silicon wafer was then peeled away from the glass revealing a gold template of the silicon surface with a roughness below 3 nm/μm<sup>2</sup>. The commercial Si<sub>3</sub>N<sub>4</sub> cantilevers (Digital Instruments) were coated with 100 nm of gold by thermal evaporation following a 10-nm adhesion layer of chromium.

**Substrate and Tip Modification.** Monolayers of 11-thioundecyl-1-phosphonic acid were formed by immersion of the gold-coated substrates and tips immediately after preparation in 0.1–0.5 mM ethanol solution containing the SAM molecules for 2 and 24 h at room temperature, respectively. Upon removal from solution, the modified tips and substrates were rinsed extensively with absolute ethanol and finally with distilled water (pH 7) before use.

**Chemical Force Microscopy (CFM) and Adhesion Measurements.** Adhesion measurements were made with a Molecular Imaging picoSPM, equipped with a flow cell and controlled by Nanoscope IIIa electronics (Digital Instruments). Modified tips were rinsed in ethanol and dried under N<sub>2</sub> just prior to mounting them in the flow cell. All measurements were carried out with a

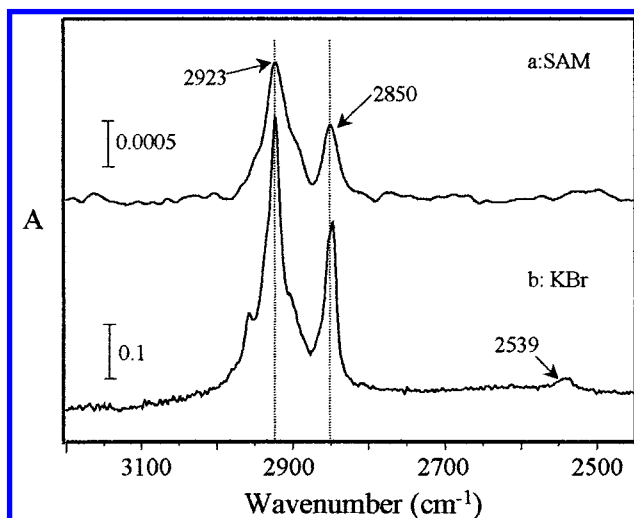


Figure 1. FT-IR spectra of (a) 11-thioundecyl-1-phosphonic acid SAM and (b) the same material in a KBr pellet.

40 μm × 40 μm scanner and thin, long (200 μm) Si<sub>3</sub>N<sub>4</sub> cantilevers (DI Instruments) at room temperature. The adhesive interaction between phosphate SAM modified tips and substrates was determined by recording force versus displacement curves under conditions of varying pH in a phosphate buffer.

The force–displacement curve plots the cantilever deflection (or force when calibrated using the cantilever spring constant) versus sample displacement. A full cycle of tip approach, contact, and retraction from the sample is recorded. The point at which the tip separates from the sample is called the pull-off point. The pull-off force at the pull-off point corresponds to the adhesion force between the tip and sample. Average adhesion force values were determined from at least 100 individual force curves at each pH value. All force versus displacement curves were captured using Nanoscope III software and later analyzed on a PC using custom software.

**RESULTS AND DISCUSSION**

The degree of order within the phosphate SAMs was determined by reflection absorption FT-infrared spectroscopy (Bruker IFS48 RA FT-IR spectrometer equipped with a SPECAC variable-angle reflection accessory). The spectra of the 11-thioundecyl-1-phosphonic acid SAM and the same material in a KBr pellet in the frequency region 3200–2450 cm<sup>-1</sup> are shown in Figure 1 a and b, respectively.

The first feature of note in the SAM spectrum is the absence of the absorption due to the S–H stretch ( $\nu(\text{S–H})$ ), which, for an isotropic sample, gives rise to a peak<sup>25</sup> around 2539 cm<sup>-1</sup>. The disappearance of  $\nu(\text{S–H})$  is generally attributed to the formation of the gold–sulfur bond in such systems and is strong evidence that the SAM molecules are covalently linked to the gold surface in the manner predicted. The second feature of importance is the presence of the asymmetric and symmetric CH<sub>2</sub> stretching vibrations observed at the same frequency in both the SAM and

(24) Wagner, P.; Hegner, H.; Guntherodt, H.-J.; Simenza, G. *Langmuir* **1995**, *11*, 3867–3875.

(25) Lin-Vien, D.; Colthup, N. B.; Fateley, W. G.; Grasselli, J. G. *The Handbook of Infrared and Raman Characteristic Frequencies of Organic Molecules*; Academic Press: New York, 1991.

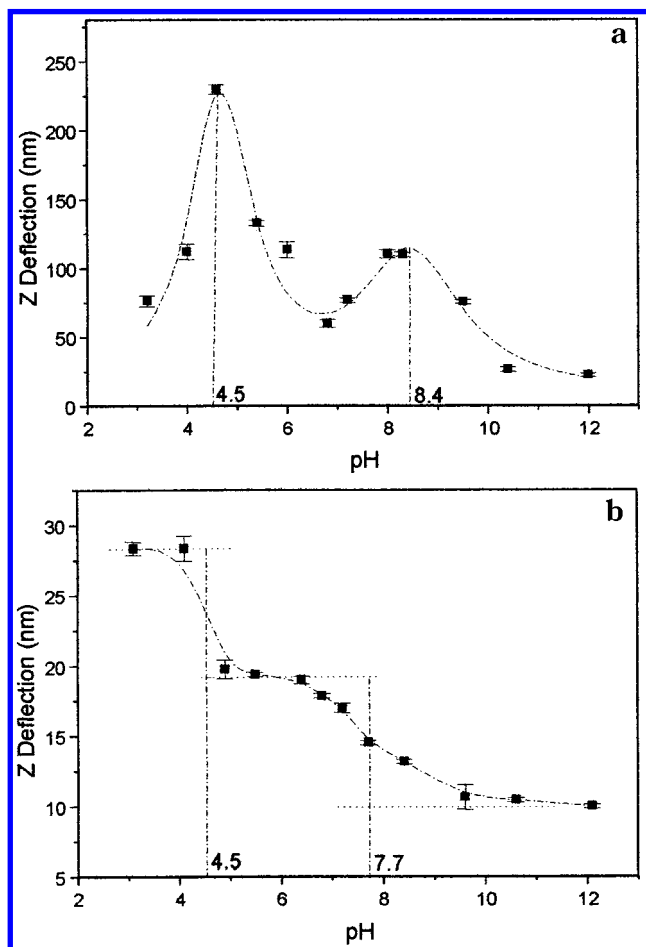


Figure 2. Force titration curve of 11-thioundecyl-1-phosphonic acid modified tip and substrate in phosphate buffer at ionic strengths: (a)  $10^{-4}$  and (b)  $10^{-1}$  M.

KBr pellet at  $2923$  and  $2850\text{ cm}^{-1}$ , respectively.<sup>25</sup> Snyder et al.<sup>26</sup> demonstrated that the peak positions of  $\text{CH}_2$  stretching modes are sensitive indicators of the degree of packing of the polyethylene chains. In our sample, according to their analyses, the peak positions imply that the alkyl chains exhibit quite a high packing density similar to that of a monolayer of decanethiol. The disappearance of  $\nu(\text{P}=\text{O})$  at  $1140\text{ cm}^{-1}$  in the SAM spectrum compared with the KBr measurement suggests that the headgroups form an ordered layer in which the phosphonyl group is possibly involved in intramonolayer hydrogen bonding. We tentatively propose a model for the SAM structure in which one of the hydroxyl groups is in the plane of the SAM and is involved in in-plane hydrogen bonding with a phosphonyl group, and the other lies out of the plane of the monolayer. The form of the force titration curves can be explained well using this model but further detailed characterization of this novel SAM is required and is presently underway.

Figure 2 shows the force (deflection) titration curves obtained using tip and substrate both modified with the phosphonic acid SAM in buffers of low ( $10^{-4}$  M) (a) and high ( $10^{-1}$  M) (b) ionic strength. At low ionic strength, the force titration curve consists of two peaks at pH 4.5 and pH 8.4. However, at higher ionic

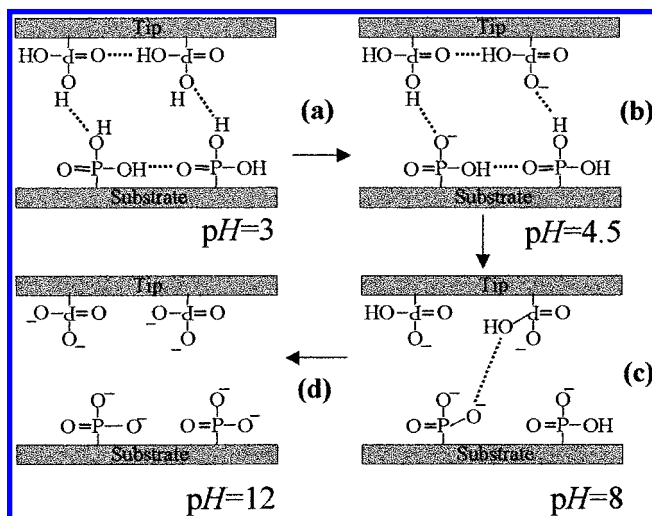


Figure 3. Schematic representation of the proposed interactions of 11-thioundecyl-1-phosphonic acid modified tip and substrate in  $10^{-4}$  M phosphate buffer at different pH values: (a) 3, (b) 4.5, (c) and (d) 12.

strength, the force titration curve takes the form of two monotonic steps to lower adhesion as the pH is increased.

In the case of the low ionic strength force titration (Figure 2a), the curve can be explained in terms of hydrogen bonding and electrostatic repulsion as shown in Figure 3.

At the low pH values, uncharged  $\text{PO}(\text{OH})_2$  groups dominate both the tip and substrate and the finite adhesion in this region can be attributed to hydrogen bonding between the two out-of-plane hydroxyl groups (Figure 3a).<sup>7,27</sup> The in-plane groups may experience some competition between forming intra- and intermonolayer hydrogen bonds when the tip contacts the substrate, but it is likely that the out-of-plane groups dominate the adhesion at this pH. Large distortions of the SAM structure upon contact of the two surfaces would lead to exposure of the hydrophobic alkyl chains. This would lead to strong hydrophobic forces, which would dominate the interaction of the two surfaces,<sup>1</sup> and we do not observe such an effect. The low-pH peak corresponds to the ionization of the out-of-plane hydroxyl groups, and the increase in measured adhesion under low ionic strength conditions is probably due to the formation of stronger hydrogen bonds between neutral OH groups and negatively charged  $\text{O}^-$  deprotonated species (Figure 3b). We assume that the peak in the adhesion force in Figure 2a at pH 4.5 corresponds to the point where 50% of the out-of-plane groups are ionized since this would be expected to maximize the number of stronger hydrogen bonds formed between tip and sample. The position of this peak therefore corresponds to the  $\text{p}K_a$  of the first group. As the pH increases beyond pH 4.5, more than 50% of the groups become ionized, the number of out-of-plane OH groups is reduced, and fewer of the bonds can form. The electrostatic repulsion between the ionized groups on tip and sample must also contribute to the reduction in the measured adhesion.

As the pH is increased further, the in-plane OH group is deprotonated. The rise in measured adhesion must be due to a few even stronger bonds between neutral groups on one surface

(26) Snyder, R. G.; Maroncelli, M.; Strauss, H. L.; Halknark, C. A. *J. Phys. Chem.* **1986**, *90*, 5623–5630.

(27) Van der Vegte, E. W.; Hadziioannou, G. *J. Phys. Chem. B* **1997**, *101*, 9563–9569.



and two O<sup>-</sup> groups (Figure 3c). The magnitude of the second peak is less than the first due to the fact that fewer such bonds can be formed but also due to the increased repulsion from two net negatively charged surfaces. Again it appears reasonable that the position of the second peak (pH 8.4) is at the pH where 50% of these groups are ionized and therefore corresponds to the p*K*<sub>a</sub>. Finally, as the pH increases beyond 8.4, the majority of the surface groups of our phosphate-terminated SAM are ionized (Figure 3d), leading to a net repulsive force between the tip and sample, and the adhesion falls toward zero.

When a high ionic strength buffer was used (Figure 2b), the shape of the force titration curve changed to that of two sigmoidal step functions, analogous to the shape observed for carboxylic acid SAMs in high ionic strength buffers.<sup>7</sup> The shape of the force titration curve for phosphate in high ionic strength buffers can be explained in terms of the effects of the formation of an electric double layer at the surface of the SAM as the headgroups are ionized. The adhesion force value at pH <4 can be attributed to hydrogen bonding between the two neutral phosphate surfaces and is of similar magnitude at high and low ionic strength. The formation of electric double layers on the two surfaces under high ionic strength conditions prevents the formation of hydrogen bonds between O<sup>-</sup> and OH groups which we have suggested are responsible for the peak in the adhesion force at low ionic strengths. The adhesion force therefore falls as the out-of-plane hydroxyl groups ionize due to the repulsion between the two electric double layers and the reduction in number of neutral OH groups for hydrogen bonding. The formation of the double layer continues as the second OH group is ionized and the adhesion falls toward zero.

Previous studies<sup>6,7</sup> have used Johnson–Kendall–Roberts (JKR) theory<sup>28</sup> to derive the surface p*K*<sub>a</sub> from the high ionic strength force titration. The adhesion force between the tip and substrate is given by JKR theory to be

$$F_{\text{ad}} = (3/2)\pi R(\gamma_s + \gamma_t - \gamma_{\text{st}}) \quad (1)$$

where  $\gamma_s$  and  $\gamma_t$  are the surface free energies of the tip and sample and  $\gamma_{\text{st}}$  is the interfacial free energy of the two contacting surfaces. If the tip and sample have the same surface functional groups, then clearly  $\gamma_{\text{st}} = 0$  and  $\gamma_s = \gamma_t$ , and it is possible to simplify the eq 1 by setting  $\gamma_s = \gamma_t = \gamma$ , where  $\gamma$  is the free energy of the surface in equilibrium with solvent,

$$F_{\text{ad}} = 3\pi R\gamma \quad (2)$$

The total surface free energy,  $\gamma$ , comprises two components: a contribution from the ionized groups and one from the neutral groups in the surface. Equation 2 can therefore be rewritten as,

$$F_{\text{ad}} = 3\pi R[(1 - \beta)\gamma_{\text{HB}} + \beta\gamma_{\text{B}^-}] \quad (3)$$

where  $\beta$  is the fraction of surface groups that are ionized and  $\gamma_{\text{B}^-}$  and  $\gamma_{\text{HB}}$  are the surface free energy of completely a deprotonated and a neutral surface, respectively. When half the surface groups are ionized,  $\beta = 1/2$  and therefore we can define the adhesion force that corresponds to this value  $F_{1/2}$  as,

$$F_{1/2} = 3\pi R \frac{1}{2}(\gamma_{\text{HB}} + \gamma_{\text{B}^-}) \quad (4)$$

According to this model the maximum adhesion force occurs for two neutral surfaces when hydrogen bonding is at a maximum, and the minimum adhesion force occurs when both surfaces are completely ionized and electrostatic repulsion dominates. Therefore eq 4 can be rewritten,

$$F_{1/2} = (1/2)(F_{\text{ad}}(\text{max}) + F_{\text{ad}}(\text{min})) \quad (5)$$

The p*K*<sub>a</sub> of the surfaces is therefore given as halfway between the maximum and minimum adhesion, i.e., the midpoint of the step.

Our data therefore suggest that the surface p*K*<sub>a</sub>s of the two groups are 4.5 and 7.7. JKR theory does not predict the effect of the ionic strength on the shape of the force titration or the fact that the pH of the midpoints of the steps and the positions of the peaks are not the same. The problem with JKR theory may derive from the fact that it is a macroscopic theory not a microscopic one. The area of contact must be macroscopic (semi-infinite) so that the interfacial free energy is simply given by a single parameter,  $\gamma$ , appropriate to the surface materials. In the micro- or nanoscopic regime, several other factors should be taken into account: (a) the dispersion interactions (Hamaker/Lifshitz) between tip and sample depend on the geometry of the tip;<sup>29</sup> (b) the sample molecular surface may partly melt and wet the tip; and (c) specific molecular interactions (which do not rule out the use of JKR theory on macroscopic surfaces since the work of adhesion is still correctly defined) could be dependent on tip geometry and surface roughness.

Further work is necessary and underway using a range of different SAM headgroups to elucidate this problem.

## CONCLUSION

We have reported on the synthesis of a novel phosphonic acid  $\omega$ -functionalized alkanethiol and the formation of self-assembled monolayers on gold. Preliminary characterization suggests that an ordered monolayer is formed with one of the hydroxyl groups involved in hydrogen bonding within the monolayer. The ionization state of this diprotic acid was determined as a function of ionic strength by measuring force titration curves using the atomic force microscope.

In low ionic strength buffers, the ionization of the two hydroxyl groups results in the presence of two peaks in the force titration curve at pH values of 4.5 and 8.4, slightly higher than the measured p*K*<sub>a</sub> values for this group free in solution. The peaks in the adhesion force titration at low ionic strength are tentatively attributed to increased hydrogen bond strength between ionized and neutral groups on the tip and substrate and the competition between hydrogen bonding and electrostatic repulsion of two net negatively charged surfaces.

At high ionic strength, the attractive interaction between tip and sample was dramatically reduced by the formation of an

(28) Johnson, K. L.; Kendall, K.; Roberts, A. D. *Proc. R. Soc. London, A* **1971**, *324*, 301–313.

(29) Helm, C. A.; Iisraelachvili, J. N.; McGuigan, P. M. *Science* **1989**, *246*, 919–923.

electric double layer and the shape of the force–titration curve was dramatically altered. If JKR theory is applied at high ionic strength, then the measured surface  $pK_a$  values (corresponding to the force halfway between the neutral and fully deprotonated states) are close to those measured at low ionic strength. However, JKR theory does not predict the shape of the force titration curve under low ionic strength conditions, and further work is necessary to develop a satisfactory model for the force titration behavior under these conditions.

#### ACKNOWLEDGMENT

The authors thank the Biotechnology and Biological Science Research Council of England for financial support.

Received for review November 15, 1999. Accepted February 22, 2000.

AC9913107